e-Prime - Advances in Electrical Engineering, Electronics and Energy 9 (2024) 100692

Contents lists available at ScienceDirect

e-Prime - Advances in Electrical Engineering, Electronics and Energy

journal homepage: www.elsevier.com/locate/prime

Frequency stabilization in microgrid with PV system based on maximum power extraction: A sliding mode approach

Ark Dev [a,*], Gautam Sarvaiya [b], Bharti Parmar [b], Urvashi Chauhan [c]

[a] Department of Electrical Engineering, Parul Institute of Engineering and Technology, Parul University, Vadodara, Gujarat, India
[b] Department of Electrical Engineering, Lukhdhirji Engineering College, Morbi, Gujarat, India
[c] Department of Electronics and Communication Engineering, KCC Institute of Technology and Management, Greater Noida, Uttar Pradesh, India

ARTICLE INFO

Keywords:
Frequency stability
Microgrid (MG)
Maximum power point tracking (MPPT),
Sliding mode control (SMC)

ABSTRACT

The article addresses the critical issue of frequency regulation in microgrids (MG) integrated with solar photovoltaic (PV) systems, which rely on maximum power point tracking (MPPT) using sliding mode control (SMC). The frequency stability of MGs is a significant concern due to the inherent variability of renewable energy sources, making frequency regulation challenging. This research proposes a dual-objective control strategy. Firstly, it ensures the solar PV system maximizes power extraction via a buck-boost converter controlled by SMC. Simultaneously, it maintains frequency regulation in the MG under load disturbances using SMC. The SMC technique guarantees precise convergence to the maximum power operating point and minimizes frequency deviations in the MG. The proposed solution demonstrates effective maximum power extraction under varying irradiance levels and reliable frequency regulation despite system parameter uncertainties and nonlinearities such as generation rate constraints (GRC) and governor deadband (GDB). Additionally, the SMC-based design achieves faster convergence compared to traditional proportional-integral (PI) controllers optimized using intelligent techniques. Stability analysis, performed using Bode and Nyquist plots, further confirms the robustness of the proposed system. The model was developed and tested in the MATLAB Simulink environment, showcasing its efficacy and reliability.

1. Introduction

Energy serves as a crucial instrument in the swiftly evolving world. The unchecked surge in energy demand has contributed to the depletion of fossil fuel reserves. Major energy sources like coal, oil and solid biomass has underpinned the growth and expansion of energy sector. As a result, the energy sector worldwide is witnessing a paradigm shift from conventional to unconventional energy sources. Alternative energy sources such as solar, wind, hydro, tidal, and geothermal are cost-effective, environmentally friendly, dependable, and replenishable at a faster pace than their consumption. Renewable energies based MGs have been found as an important part of this dramatic transition from conventional to renewable energy resources. A MG is a localized energy system that integrates distributed energy resources, such as renewable sources, generators, and energy storage, to supply electricity to a specific area or community [1,2]. Microgrids (MGs) are contemporary, dependable, and commonly seen as compact electrical power distribution systems. Renewable energy-powered MGs encompass a variety of sources including solar photovoltaics (PVs), wind turbine generators (WTGs), diesel engine generators (DEGs), fuel cells (FCs), battery energy systems (BESs), and flywheel energy systems (FES). These sources are clean and widely available. Nonetheless, the inherent unpredictability of solar irradiation and wind speed has consistently raised concerns among researchers and control engineers regarding the frequency stability of MGs. Furthermore, devising methods to secure the optimal operation of solar PV systems for maximal power extraction during sunlight hours would offer an additional advantage in this field. In the sequence, a comprehensive literature review is provided, highlighting key contributions in the field, identifying existing gaps and motivations, and presenting the main contributions of the current work.

1.1. Literature survey

Literature in this field has revealed that MPPT for PV system can be broadly classified into three different categories: classical, intelligent and optimized. Classical MPPT techniques such as incremental

* Corresponding author.
E-mail address: arkdev.014@gmail.com (A. Dev).

https://doi.org/10.1016/j.prime.2024.100692
Received 22 August 2023; Received in revised form 14 July 2024; Accepted 15 July 2024
Available online 20 July 2024

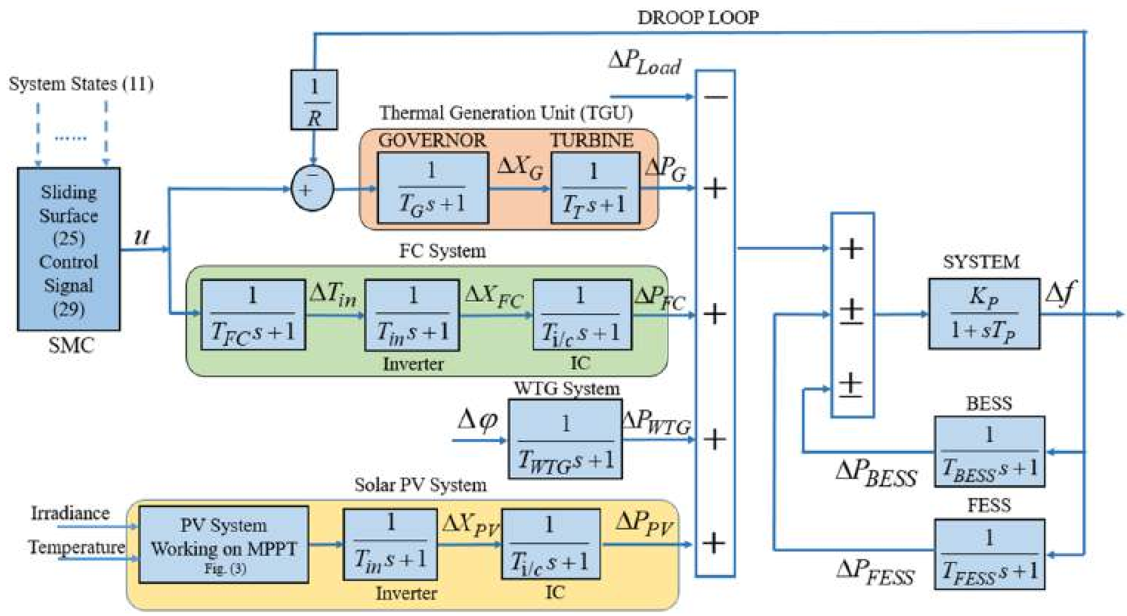

Fig. 1. Load Frequency Control Modeling of MG [1,20].

conductance MPPT [3,4], perturb and observe (P&O) MPPT technique [5,6], hill climbing MPPT [7], fraction of open circuit voltage [8] and short circuit current techniques [9] are widely used techniques due to their simple and easy implementation. However, these algorithms suffer from poor tracking efficiency, slow response, rapid oscillation around maximum power point which results in loss of power. Intelligent MPPT techniques such as artificial neural network (ANN) [10,11], fuzzy logic controller [12,13], adaptive neuro fuzzy [14] are present in literature. Although, these algorithms are dedicated for dynamic weather changing condition and high tracking speed, but they suffer from huge control circuit complexity and big data processing requirements. Optimization based procedure such as Particle Swarm Optimization (PSO) [15], Grey Wolf Optimization (GWO) [16], Cuckoo search [17], Ant Colony [18], Artificial Bee Colony (ABC) [19] have been found to be effective and feasible to apply without the knowledge of PV panel parameters.

As far as frequency stability in MGs is concerned, classical control techniques such as PI, PID controllers [20-22], fractional order PI controller cascaded with a fractional order tilt-derivative controller [23] are widely used which provides an additional non-integer integro-differential order selection compared to traditional PID controller. These controllers being simple in design are affected by poor transient behavior. The optimal gain selection of PI/PID controllers based on soft computing approaches and metaheuristic optimization approaches such as Artificial Neural Network (ANN) [24], Adaptive Neuro-Fuzzy [25], Particle Swarm Optimization (PSO) [26], Dragonfly Algorithm (DA) [27], Ant Lion [28], Manta Ray Foraging (MRF) [29], Fuzzy logic [30], PSO based ANN [31], PSO based Fuzzy [32], Teaching Learning (TL) optimization based SMC [33] is well-documented in the literature. A novel heuristic algorithm combining type-2 fuzzy logic sets and the modified harmony search algorithm is proposed for LFC strategy for MGs considering electric vehicles (EVs) [34]. Similar works comprising of heuristic optimization based intelligent and robust controllers like 2DOF state feedback PI controller, cascade fractional order PI- fractional order proportional tilt integral derivative (PTID) with energy storage devices for AGC performance in electric power systems are reported in [35,36] respectively. Model predictive control (MPC) for MG frequency stabilization is reported in [37-39]. Optimal controllers utilizing energy storage devices for multi area power systems under deregulated environment is proposed in [40]. Advancement and development in robust control strategies have ensured the usage of SMC,H_∞controllers, μ-synthesis controllers for frequency regulation in MGs [1,41-45]. The concept of event triggering based SMC approach for frequency regulation in MG is presented in [46]. Readers are encouraged to go through the state of the art review on modern and future developments in AGC/LFC of conventional and renewable energy based power systems [47].

1.2. Motivation

As evidenced by investigations into reported works in the field, the exploration of SMC for frequency regulation in MGs, coupled with maximum power extraction, remains a growing area of research. The SMC is particularly appealing due to its benefits, including faster convergence, robustness against disturbances, and simplicity in design, making it a promising approach for ongoing and future studies in this domain. Within the MG system, two frequency control loops exist: primary and secondary control. The primary control employs droop control, a fixed gain mechanism. However, this approach alone lacks the capacity to effectively stabilize frequency in the face of load disturbances and uncertain energy sources. Consequently, a secondary control strategy is introduced, utilizing sliding mode techniques to enhance system robustness in the presence of disturbances and uncertainties. In addition, unlike a boost converter for MPPT, a buck-boost converter provides greater versatility and flexibility to adapt to varying conditions, ensuring consistent performance and optimal power extraction.

1.3. Contribution

In this study, an attempt is made to address frequency stability in MGs where in solar PV system is working on maximum power extraction using sliding mode. The fundamental objectives of the work are listed below:

- Design of the MPPT controller via sliding mode for maximum power extraction from solar PV system integrated with MG system.
- Sliding mode load frequency stabilization $\left(\underset{t\to\infty}{\Delta f(t)} = 0\right)$ under load disturbance, intermittent nature of solar irradiation, and wind disturbance by satisfying, $\sum P = \Delta P_G + \Delta P_{FC} + \Delta P_{WTG} + P_{PV} \pm \Delta P_{BESS} \pm \Delta P_{FESS} - \Delta P_{Load} = 0$.

In addition, the robustness of the proposed design is validated under

Table 1
Proposed model variable description.

Variables	Description
Δf	Frequency deviation (Hz)
ΔP_{FESS}	Change in flywheel energy storage power output (p.u.)
ΔP_{BESS}	Change in battery energy storage power output (p.u.)
ΔP_G	Change in diesel engine generator power output (p.u.)
ΔX	Change in governor valve position (p.u.)
ΔP_{FC}	Change in fuel cell power output (p.u.)
ΔP_{PV}	Change in PV system power output (p.u.)
ΔP_{WTG}	Change in wind turbine generator power output (p.u.)
ΔP_{LOAD}	Change in load (p.u.)
u	Control input to MG

random changes in load and solar irradiance, system parameter uncertainties, and nonlinearities. It is observed that the frequency deviation is found to be well within acceptable limits. The system stability is studied in frequency domain using Bode and Nyquist plots highlighting closed loop system stability under wide range of operating conditions. The frequency regulation achieved by the proposed method is also observed to be superior compared to commonly used PI and PID controllers tuned using soft computing optimization approaches such as Ziegler Nichols, ANN-GA methods [20], PSO [26], DA [27], ALO [28], and MAF optimization [29].

1.4. Outline

The remaining paper is outlined as follow: In Section 2, LFC modeling of MG and control objectives are defined. In Section 3, controller design for MPPT and frequency regulation in MG is discussed. Section 4 deals with simulation results, discussion and comparison with recent reported works in MG using conventional PI and PID controllers. Finally, few conclusions are drawn in Section 5 along with scope for future work.

2. Microgrid: modeling and control objectives

Fig. 1 depicts load frequency modeling of MG. The decentralized resources such as thermal generating units and wind turbine generators (WTGs) are linked to the AC bus through power electronic devices, which ensure synchronization of the AC sources. Additionally, these power electronic devices serve the purpose of converting DC to AC for sources like photovoltaic (PV) panels and fuel cells (FCs). Moreover, a battery energy storage (BES) system is integrated with the AC bus via a power electronics converter, facilitating the conversion of AC to DC during charging and DC to AC during discharging. As this study focuses exclusively on the frequency regulation control methodology, the consideration of power electronic devices falls beyond its scope. Readers are advised to consult reference [48] for a comprehensive understanding of power electronic converter modeling and control within MG applications. The subsequent section outlines the state dynamics of the MG system, while Table 1 presents the system's proposed model variables.

$$\Delta\dot{f} = -\frac{1}{T_P}\Delta f + \frac{K_P}{T_P}[\Delta P_{PV} + \Delta P_{WTG} + \Delta P_{FC} + \Delta P_G \pm \Delta P_{BESS} \pm \Delta P_{FESS} - \Delta P_{LOAD}] \tag{1}$$

$$\Delta\dot{P}_{FESS} = -\frac{\Delta P_{FESS}}{T_{FESS}} + \frac{\Delta f}{T_{FESS}} \tag{2}$$

$$\Delta\dot{P}_{BESS} = -\frac{\Delta P_{BESS}}{T_{BESS}} + \frac{\Delta f}{T_{BESS}} \tag{3}$$

$$\Delta\dot{P}_G = -\frac{\Delta P_G}{T_t} + \frac{\Delta X_G}{T_t} \tag{4}$$

$$\Delta\dot{X}_G = -\frac{\Delta f}{RT_G} - \frac{\Delta X_G}{T_G} + \frac{u}{T_G} \tag{5}$$

$$\Delta\dot{P}_{FC} = -\frac{\Delta P_{FC}}{T_{1/c}} - \frac{\Delta X_{FC}}{T_{1/c}} \tag{6}$$

$$\Delta\dot{X}_{FC} = -\frac{\Delta X_{FC}}{T_{in}} + \frac{\Delta T_{in}}{T_{in}} \tag{7}$$

$$\Delta\dot{T}_{in} = -\frac{\Delta T_{in}}{T_{FC}} + \frac{u}{T_{FC}} \tag{8}$$

$$\Delta\dot{P}_{WTG} = -\frac{1}{T_{WTG}}\Delta P_{WTG} + \frac{1}{T_{WTG}}\Delta\varphi \tag{9}$$

$$\Delta\dot{P}_{PV} = -\frac{1}{T_{i/c}}\Delta P_{PV} + \frac{1}{T_{i/c}}\Delta X_{PV} \tag{10}$$

Rewriting Eqs. (1)-(8) in matrix form [23,39,43],

$$\begin{aligned}\dot{X}(t) &= AX(t) + Bu(t) + Dd(t)\\ y(t) &= CX(t)\end{aligned} \tag{11}$$

where $X^{(8\times1)} = [\Delta f\ \Delta P_{FESS}\ \Delta P_{BESS}\ \Delta P_G\ \Delta X_G\ \Delta P_{FC}\ \Delta X_{FC}\ \Delta T_{in}]^T$,$A^{(8\times8)}$, $B^{(8\times1)}$, $C^{(1\times8)}$and $D^{(8\times1)}$ represent state, system, input, output and disturbance matrices respectively.

Rewriting (11) in augmented form as,

$$\begin{bmatrix}\dot{x}_1(t)\\ \dot{x}_2(t)\end{bmatrix} = \begin{bmatrix}A_{11} & A_{12}\\ A_{21} & A_{22}\end{bmatrix}\begin{bmatrix}x_1(t)\\ x_2(t)\end{bmatrix} + \begin{bmatrix}B_1\\ B_2\end{bmatrix}u(t) + \begin{bmatrix}D_1\\ D_2\end{bmatrix}d(t) \tag{12}$$

where $X(t) = \begin{bmatrix}x_1^{(1\times1)}(t) & x_2^{(7\times1)}(t)\end{bmatrix}^T$,$A = \begin{bmatrix}A_{11}^{(1\times1)} & A_{12}^{(1\times7)}\\ A_{21}^{(7\times1)} & A_{22}^{(7\times7)}\end{bmatrix}$,$B = \begin{bmatrix}B_1^{(1\times1)}\\ B_2^{(7\times1)}\end{bmatrix}$, and $D = \begin{bmatrix}D_1^{(1\times1)}\\ D_2^{(7\times1)}\end{bmatrix}$. Writing the state dynamics for controller designs with an assumption that $|D_1 d| \le \xi$, where ξ is the known upper bound of unknown disturbance [43].

$$\left.\begin{aligned}\dot{x}_1(t) &= A_{11}x_1(t) + A_{12}x_2(t) + \xi\\ \dot{x}_2(t) &= A_{21}x_1(t) + A_{22}x_2(t) + B_2u(t)\end{aligned}\right\} \tag{13}$$

The matrices presented in Eq. (13) are provided as follows:

$$A_{11} = -\frac{1}{T_P};\ A_{12} = \begin{bmatrix}-\frac{K_P}{T_P} & -\frac{K_P}{T_P} & \frac{K_P}{T_P} & 0 & \frac{K_P}{T_P} & 0 & 0\end{bmatrix};$$

$$A_{21} = \begin{bmatrix}\frac{1}{T_{FESS}} & \frac{1}{T_{BESS}} & 0 & -\frac{1}{RT_G} & 0 & 0 & 0\end{bmatrix}^T;$$

$$A_{22} = \begin{bmatrix}-\frac{1}{T_{FESS}} & 0 & 0 & 0 & 0 & 0 & 0\\ 0 & -\frac{1}{T_{BESS}} & 0 & 0 & 0 & 0 & 0\\ 0 & 0 & -\frac{1}{T_t} & \frac{1}{T_t} & 0 & 0 & 0\\ 0 & 0 & 0 & -\frac{1}{T_G} & 0 & 0 & 0\\ 0 & 0 & 0 & 0 & -\frac{1}{T_{1/c}} & \frac{1}{T_{1/c}} & 0\\ 0 & 0 & 0 & 0 & 0 & -\frac{1}{T_{in}} & \frac{1}{T_{in}}\\ 0 & 0 & 0 & 0 & 0 & 0 & \frac{1}{T_{FC}}\end{bmatrix};$$

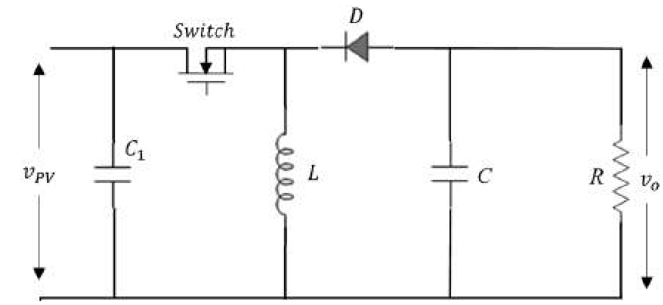

Fig. 2. Buck Boost Converter [15].

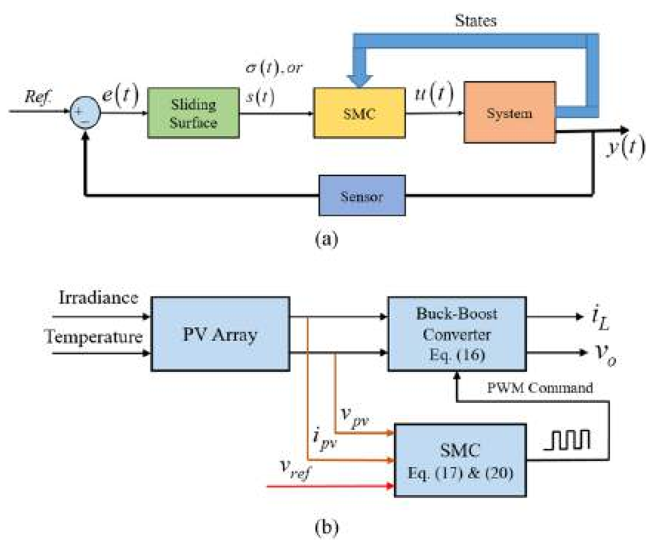

Fig. 3. Block diagram of MPPT of PV system using sliding mode [49].

$$B_1 = [0];\ B_2 = \begin{bmatrix} 0 & 0 & 0 & \frac{1}{T_G} & 0 & 0 & \frac{1}{T_{FC}} \end{bmatrix}^T;\ D_1 = \begin{bmatrix} -\frac{K_P}{T_P} \end{bmatrix};\ D_2 = \begin{bmatrix} 0 & 0 & 0 & 0 & 0 & 0 & 0 \end{bmatrix}^T.$$

3. Sliding mode controller design

3.1. MPPT using sliding mode

In recent years', solar energy received worldwide attention due to several benefits such as nature friendly, pollution free and requires less maintenance as compared to other non-conventional energy resources. The power generation using solar energy has emerged as the most promising sources among various sustainable energy sources as the systems are economically reliable. Given the significant variation in solar irradiation throughout the day, the implementation of maximum power point tracking (MPPT) control becomes crucial for optimizing the extraction of maximum power from the installed solar capacity. To compensate the effect of uncertain solar irradiation, DC-DC buck-boost converter is used. It is one of the main components of solar PV system. A DC-DC buck-boost converter can be controlled to produce voltage larger or smaller than the input voltage. The voltage regulation is done using a pulse width modulator (PWM) which is fed by the SMC. Fig. 2 depicts the model of buck-boost converter followed by its state dynamics when switch is in ON($u^c = 1$) and OFF ($u^c = 0$) condition.

The converter dynamics when switch is ON ($u^c = 1$) and OFF ($u^c = 0$), is given by,

$$\left.\begin{aligned} \frac{di_L}{dt} &= \frac{v_{pv}}{L} \\ \frac{dv_o}{dt} &= -\frac{v_o}{RC} \end{aligned}\right\} \text{ and } \left.\begin{aligned} \frac{di_L}{dt} &= -\frac{v_o}{L} \\ \frac{dv_o}{dt} &= \frac{i_L}{C} - \frac{v_o}{RC} \end{aligned}\right\} \textit{respectively } [49]. \tag{14}$$

The averaging model of converter is given in (15) [49],

$$\left.\begin{aligned} L\dot{x}_1^c(t) &= u^c(t)v_{pv} - x_2^c(t)(1 - u^c(t)) \\ C\dot{x}_2^c(t) &= x_1^c(t)(1 - u^c(t)) - \frac{x_2^c(t)}{R} \end{aligned}\right\} \tag{15}$$

where $x^c(t) = [x_1^c \quad x_2^c]^T = [i_L \quad v_o]^T$, and $u_c$is the control signal to be designed.

The fundamental steps in the implementation of the SMC is the selection of sliding surface followed by design of control input that drives the system states from any initial condition on to the sliding surface in finite time and forces the states to remain on it thereafter. The block diagrams of a generalized implementation of the SMC and MPPT design via sliding mode is shown in Figs. 3(a) and 3(b) respectively.

The SMC is designed by first specifying the sliding surface as given below,

$$\sigma(t) = \overline{x}_2^c - x_2^c(t) \tag{16}$$

where $\overline{x}_2^c$is the desired output voltage of buck-boost converter.

$$\dot{\sigma}(t) = -\dot{x}_2^c(t) \tag{17}$$

Substituting (15) in (17),

$$\dot{\sigma}(t) = -\left\{\frac{(1 - u^c(t))x_1^c(t)}{C} - \frac{1}{RC}x_2^c(t)\right\} \tag{18}$$

Using constant rate reaching law $\dot{\sigma}(t) = -\beta\text{sgn}(\sigma(t))$ [50] in above equation,

$$u^c(t) = 1 - \frac{1}{R}\frac{x_2^c(t)}{x_1^c(t)} - \frac{C}{x_1^c(t)}\beta\text{sgn}(\sigma(t)),\ \beta > 0 \tag{19}$$

The above control input $u^c(t)$ is fed to the PWM which then controls the duty cycle of the MOSFET.

The stability of sliding mode can be ensured theoretically by selecting a Lyapunov function as,

$$V(\sigma(t)) = \frac{1}{2}\sigma^2(t) \tag{20}$$

$$\dot{V}(\sigma(t)) = \sigma(t)\dot{\sigma}(t) \tag{21}$$

Substituting (18) in (21)

$$\dot{V}(\sigma(t)) = \sigma(t)\left\{-\frac{x_1^c(t)}{C} + \frac{x_1^c(t)}{C}u^c(t) + \frac{1}{RC}x_2^c(t)\right\} \tag{22}$$

Substituting the control law (19) in (22) yields,

$$\dot{V}(\sigma(t)) = \sigma(t)\{-\beta\text{sgn}(\sigma(t))\} \tag{23}$$

The right selection of controller tuning gain β ensures $\dot{V}(\sigma(t)) < 0$, $\forall t$. This confirms that the system states always remain on the sliding surface.

3.2. Frequency regulation using sliding mode

This section is dedicated to formulating a super twisting sliding mode control (ST-SMC) strategy for enhancing frequency stability in MGs when faced with load disturbances. The ST-SMC method represents a continuous second-order sliding mode approach, which effectively addresses the issue of chattering commonly associated with traditional SMC. It achieves this by operating solely on the first derivative of the sliding surface. The ST-SMC approach encompasses three main components: the equivalent control $(u_{eq}(t))$ term derived by substituting$\dot{s}(t) =$

Table 2
MG system parameter values [43].

System Parameter	Values	System Parameter	Values
K_P	66.6 (Hz/p.u.)	$T_{i/c}$	0.004 s
T_P	11.1 Hz-s	T_{WTG}	1.5 s
T_G	0.08 s	T_{PV}	1.8 s
T_T	0.4 s	T_{BESS}	0.1 s
T_{FC}	0.26 s	T_{FESS}	0.01 s
T_{in}	0.04 s	R	3 Hz/p.u.

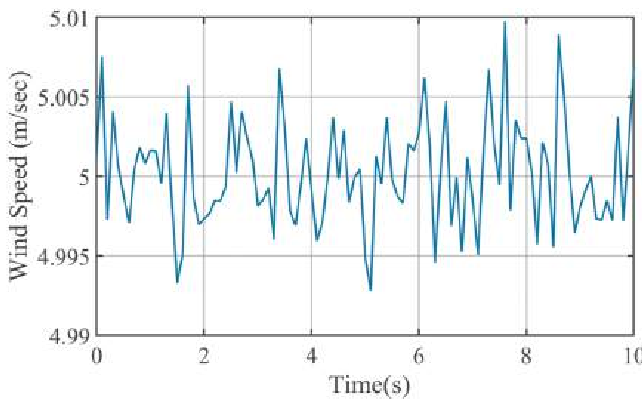

Fig. 4. Uncertain nature of considered wind speed.

Table 3
MPPT based solar PV system description and values [6,7].

Symbol	System Parameters	
	Description	*Value*
I_{sc}	Short circuit current	7.84 A
V_{oc}	Open circuit voltage	36.3 V
V_{mpp}	Voltage at maximum power point	29 V
I_{mpp}	Current at maximum power point	7.35 A
P_{mpp}	Maximum Power	213.15 W
N_{cell}	Number of cells	60
L	Inductor	10 mH
C_1	Input coupling capapcitor	400 μF
C	Output coupling capapcitor	500 μF
R	Load Resistance	100 Ω
f_{sw}	Switching frequency	10 kHz
v_{ref}	Reference output voltage	362 V
x^c	Converter system states	–
u^c	Converter control input	–

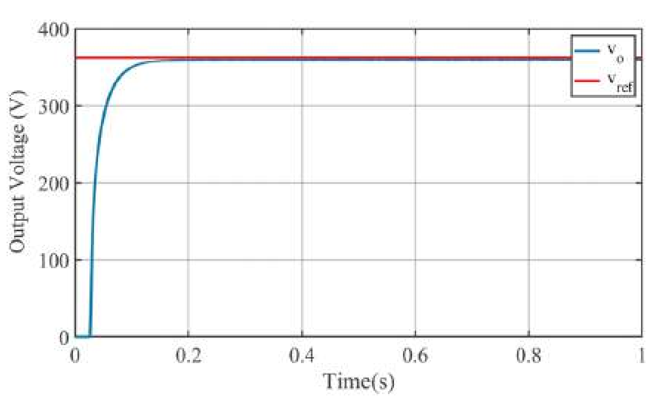

Fig. 5. Output voltage (v_o).

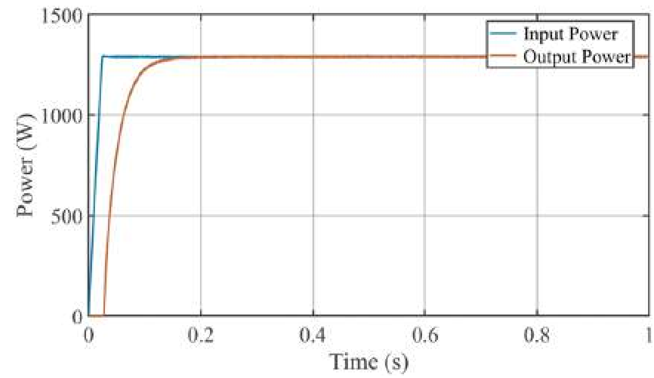

Fig. 6. Maximum power tracking with SMC.

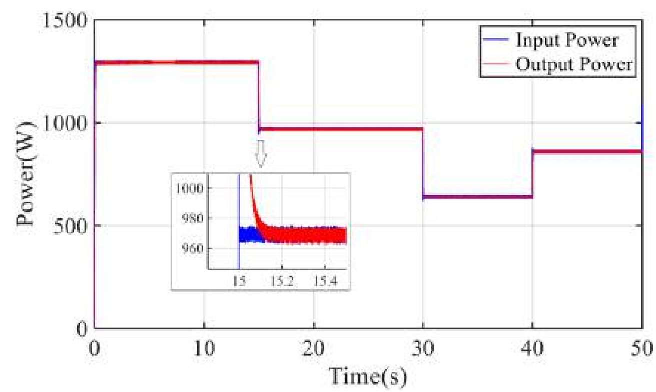

Fig. 7. Maximum power tracking with SMC with random irradiance level.

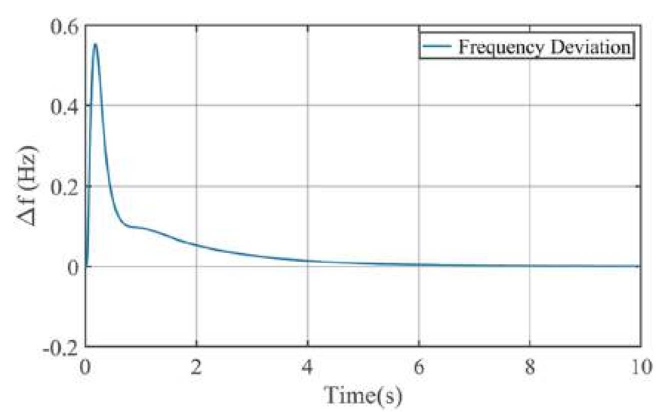

Fig. 8. Δf under step load disturbance.

0, the continuous state function, and the discontinuous state function with an integrator. The initial step in the design process involves selecting a suitable sliding surface that adopts the following structure to meet the specified control objective [43,50],

$$s(t) = \psi_1 x_1(t) + Gx_2 + \psi_2 \int_0^t x_1(t) \tag{24}$$

Here, ψ_1 and $\psi_2$represent design constants, while $G^{(1\times7)}$ signifies the gain matrix, which is subject to design to ensure that the matrix product GB_2 remains non-singular. By differentiating Eq. (24) in accordance with the dynamics outlined in Eq. (13),

$$\dot{s}(t) = \psi_1 \dot{x}_1(t) + G\dot{x}_2(t) + \psi_2 x_1(t) \tag{25}$$

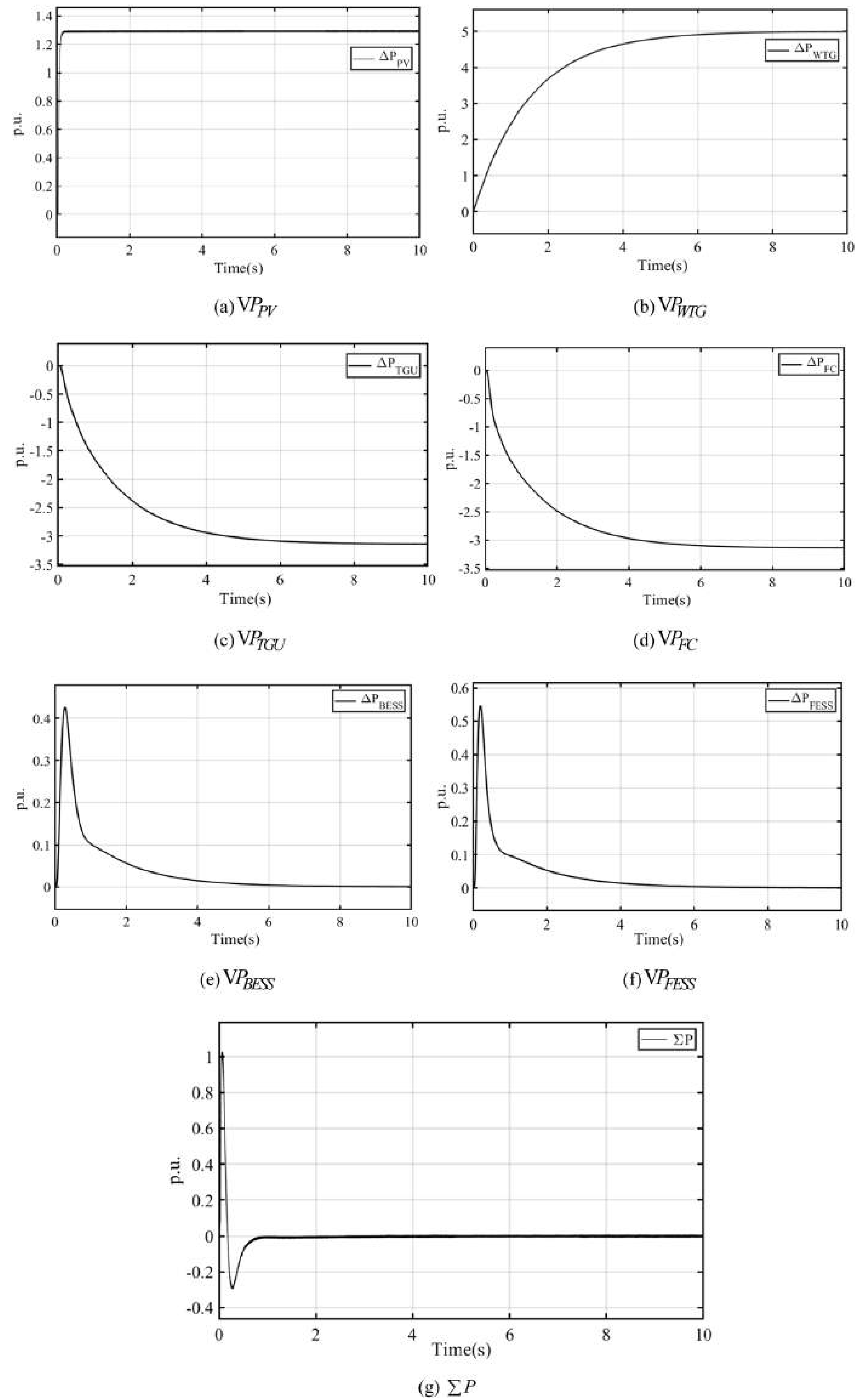

Fig. 9. Power output of all the units under step load disturbance.

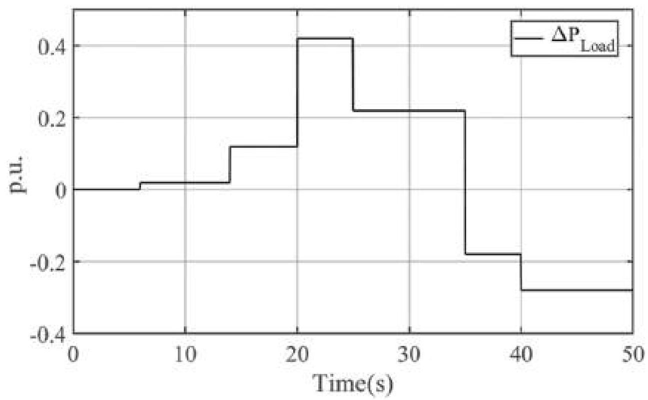

Fig. 10. Nature of random load disturbance.

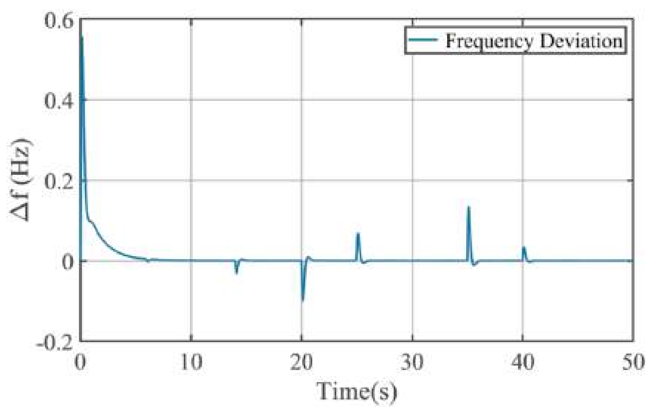

Fig. 11. $\triangle f$ under random load disturbance.

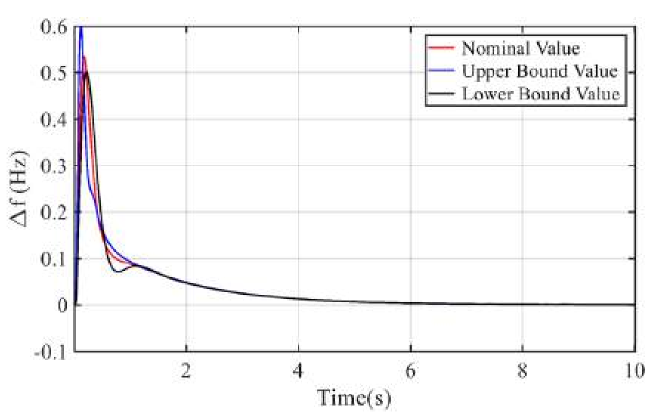

Fig. 12. $\triangle f$ with system parameter uncertainties.

Substituting (13) in (25), one can obtain,

$$\dot{s}(t) = \psi_1\{A_{11}x_1(t) + A_{12}x_2(t)\} + G\{A_{21}x_1(t) + A_{22}x_2(t) + B_2u(t)\} + \psi_2x_1(t) \tag{26}$$

Substituting $\dot{s}(t) = 0$ in (26), one can obtain equivalent control $(u_{eq}(t))$,

$$u_{eq}(t) = \frac{-1}{GB_2}\{(\psi_1A_{11} + GA_{21})x_1(t) + (\psi_1A_{12} + GA_{22})x_2(t) + \psi_2x_1(t)\} \tag{27}$$

The final control input that drives the system state to the desired trajectory and forces it to remain on it thereafter is given by [50,51],

$$u(t) = u_{eq}(t) - \alpha_1|s(t)|^{0.5}sign(s(t)) - \alpha_2\int_0^t sign(s(t))dt \tag{28}$$

where α_1, α_2 are positive constants and $\mathrm{sgn}(s(t)) = \begin{cases} 1, & s(t) > 0 \\ 0, & s(t) = 0 \\ -1, & s(t) < 0 \end{cases}$.

Recalling, $|D_1d| \leq \xi$, the constant are selected as follows: $\alpha_1 = 1.5\sqrt{\xi}$and $\alpha_2 = 1.1\xi$.

To investigate the presence of stability for the sliding surface, a Lyapunov candidate function is considered of the form,

$$V(s(t)) = \frac{1}{2}s^2(t) \tag{29}$$

Taking the derivative of (29),

$$\dot{V}(s(t)) = s(t)\dot{s}(t) \tag{30}$$

Substituting (25) in (30),

$$\dot{V}(s(t)) = s(t)\{\psi_1\dot{x}_1(t) + G\dot{x}_2(t) + \psi_2x_1(t)\} \tag{31}$$

Substituting (13) in (31),

$$\dot{V}(s(t)) = s(t)\{\psi_1(A_{11}x_1(t) + A_{12}x_2(t) + \xi) + \psi_2x_1(t) + G(A_{21}x_1(t) + A_{22}x_2(t) + B_2u(t))\} \tag{32}$$

Using the control law (28) in (32),

$$\dot{V}(s(t)) = s(t)\left\{ -\alpha_1|s(t)|^{0.5}sign(s(t)) - \alpha_2\int_0^t sign(s(t))dt + \xi \right\} \tag{33}$$

Equation (33) will always be negative i.e. $\dot{V}(s(t)) < 0$ irrespective of the $s(t)$, provided that the controller tuning gain is selected satisfying $\alpha_1 = 1.5\sqrt{\xi}$ and $\alpha_2 = 1.1\xi$. This ensures asymptotic stability and thus system states tend to zero.

4. Results and discussion

In this segment, the validity of the suggested design is affirmed through assessment within the MATLAB simulink environment, encompassing uncertain wind disturbances and load scenarios for the MG model. The MG system parameter values are given in Table 2. Fig. 4 illustrate the uncertain nature of wind speed in m/*sec* considered in MG modeling. The solar PV system and buck-boost converter system parameter values and their description is given in Table 3.

Study 1. The initial investigation involves the design of the MPPT based PV system, taking into account the operational state of irradiance 600 W/m^2 and 25 °C. The v_{PV} output from PV system act as a input to the buck-boost converter. The designed SMC provides the necessary control of duty cycle of the switch. The proposed SMC ensures that the solar PV system works on MPPT and the same is integrated to the MG system. Figs. 5 and (6) confirms the finite time convergence of output voltage and power tracking respectively. The response is free from any overshoot/undershoot and settles within acceptable limits in 0.2 s. Furthermore, the design is also validated with random changes in irradiance level. During peak hours, 600 W/m^2 irradiance level is considered which falls to 450 W/m^2at 15 s, 300 W/m^2at 30 s, further increases to 400 W/m^2at 40 s and lastly to 500 W/m^2at 50 s. Fig. 7 demonstrates that the suggested SMC guarantees MPPT even when faced with varying levels of irradiance.

Study 2. This study examines the frequency stability of the MG under load disturbances, both in the form of step changes and random fluctuations. Firstly, in the MATLAB simulink environment, at time $t = 0$ *sec*, a load shift of 5 MW is considered to have been initiated. This change in load causes frequency to deviate from its schedule value. The secondary

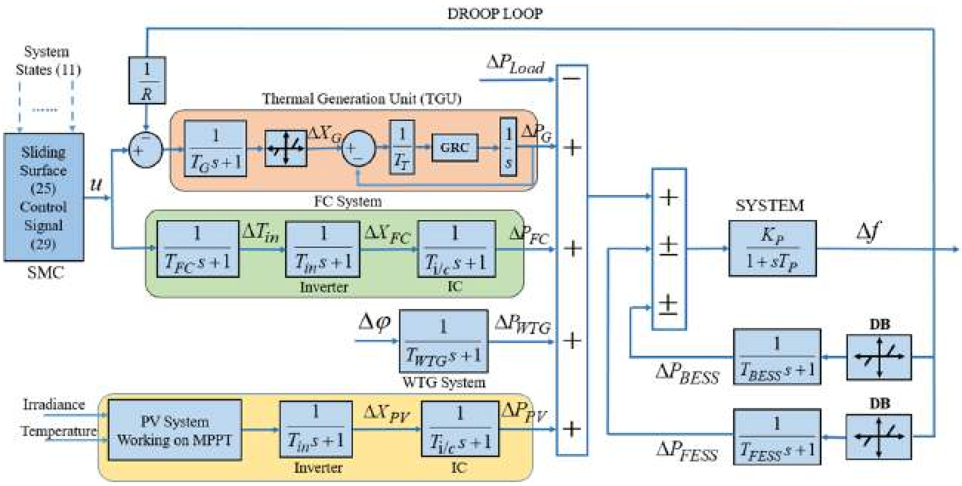

Fig. 13. MG modeling with nonlinearities.

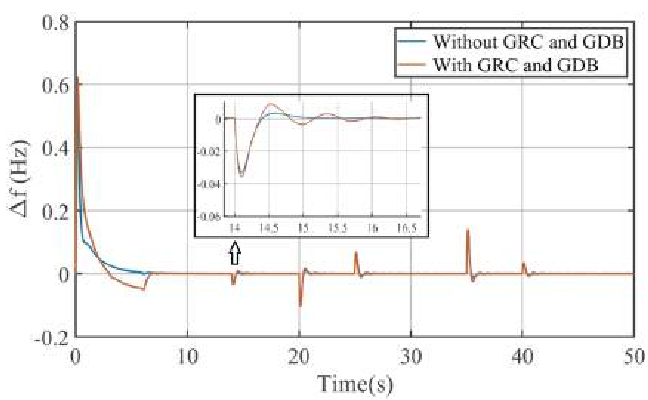

Fig. 14. Δf comparison with GRC and GDB.

control provided by the ST-SMC ensures re-stabilization of frequency after the occurrence of disturbance. The SMC's disturbance handling capability effectively mitigates the inherent uncertainties posed by renewable energy sources into the MG. Fig. 8, confirms frequency stabilization under step change in load disturbance. The power output of all the units are shown in Fig. 9. In addition, the frequency deviation is also observed with random changes in load disturbance (see Fig. 10). Fig. 11 illustrate frequency stabilization under random change in load disturbance. This affirms that the suggested design is capable of ensuring system stability even when faced with random disturbances.

Study 3. Furthermore, a robustness assessment of the proposed design is conducted, taking into account uncertainties in system parameters. The system gain (K_P), time constant(T_P), and speed regulation coefficient (R) are varied by 50 % of their nominal values. Overall, the characteristics of the MG components, the control algorithms, load characteristics, different energy storages, and the operational scenarios significantly influence the inertia, damping, and speed regulation factor of a MG model. Fig. 12 illustrate the frequency stabilization under load disturbance with system parameter uncertainties.

Moreover, the MG system is subjected to modeling including prevalent energy system nonlinearities such as GRC and GDB. The Generating Rate Constraint (GRC) represents a physical limitation on the generating unit's rate of change, while the Governor Dead Band (GDB) defines the range within which no governor action takes place [52]. In this study, GRC is assigned a value of 10 % p.u./min, and GDB is set at 0.06 %. As depicted in Fig. 13, the MG's block diagram incorporates these nonlinearities. Analysis presented in Fig. 14 illustrates that frequency deviation influenced by GRC and GDB demonstrates overshoot/undershoot behavior. Nonetheless, the proposed design effectively maintains frequency stability well within acceptable thresholds

Study 4. Stability analysis of sliding mode LFC for a MG system, using both Bode and Nyquist plots, provides comprehensive validation of system stability. The Bode plot shows a gain margin of 18.7 dB at a frequency of 16.5 rad/sec, indicating that the system can tolerate a significant increase in gain before reaching instability, thus ensuring robustness (see Fig. 15(a)). Additionally, the Nyquist plot reveals zero encirclements around the critical point $(-1,\ 0)$ and no open-loop poles in the right half of the complex s-plane. This indicates that there are no closed-loop poles in the right half of the s-plane, thereby confirming the stability of the closed-loop system (see Fig. 15(b)). The combined use of Bode and Nyquist plots not only affirms the stable operation of the sliding mode LFC in the MG system but also demonstrates its capacity to maintain frequency stability under varying operational conditions.

Study 5. Lastly, the proposed design is compared with commonly used PI and PID controller tuned using Ziegler Nichols, ANN-GA methods [20], PSO [26], DA [27], ALO [28], and MAF optimization [29]. The comparison is done considering similar system parameters in the presence of uncertainties and disturbance. It can be seen from Fig. 16 that the frequency deviation obtained using PI and PID controllers is affected by poor settling time and larger overshoot/undershoots. The fixed structure of PI and PID controllers are unable to tackle the random varying uncertainties. Whereas, the proposed SMC technique results in faster frequency stabilization under load disturbance with better transient behavior.

5. Conclusion

In this work, frequency stabilization in MG is reported using sliding mode. Maintaining frequency stability within an AC microgrid is crucial, as it guarantees the consistent and synchronized operation of interconnected power sources, enabling efficient energy distribution and safeguarding the reliability of the entire system. In the MG system modeling, the PV system integrated with the MG is ensured to be operating at the maximum power extraction. The two control objectives of MPPT tracking and frequency stabilization under uncertainties and disturbance is achieved using the SMC. Analysis of simulation outcomes reveals the robust capability of the SMC to withstand extensive uncertainties and disturbances within the system. The frequency deviation remains comfortably within acceptable thresholds, even amidst random

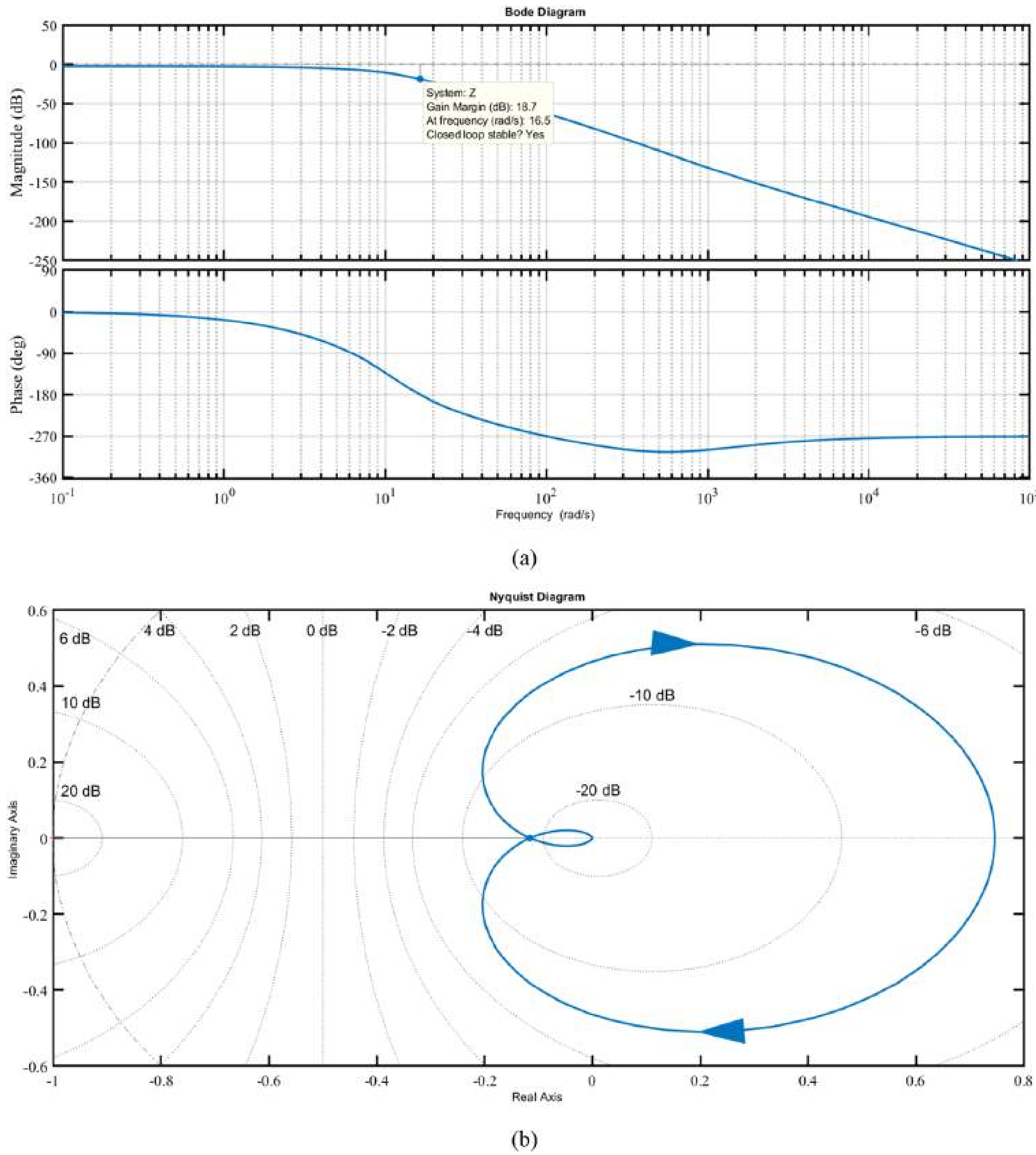

Fig. 15. Stability analysis.

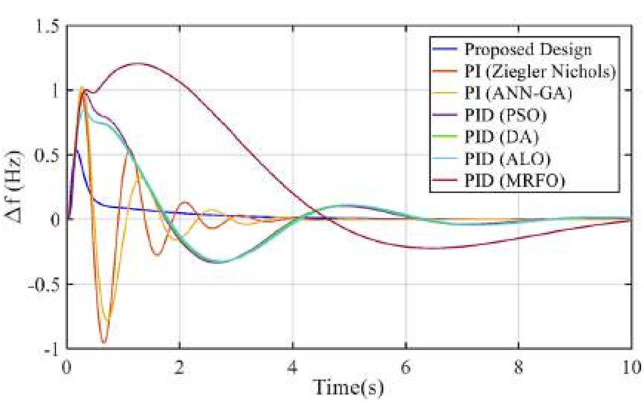

Fig. 16. Frequency deviation comparison.

load disturbances, uncertainties in system parameters, and inherent nonlinearities of energy systems. Furthermore, this study demonstrates that the proposed approach achieves swifter frequency stabilization compared to conventional PI and PID controllers tuned through AI methods.

In future, the frequency stability of MG can be studied considering cyber-attacks in form of time delays, false data injection, their detection and real time estimation.

Ethical approval

Not Applicable.

Funding

No external funding was received for this research/project.

CRediT authorship contribution statement

Ark Dev: Conceptualization, Investigation, Methodology, Software, Supervision, Writing – original draft. **Gautam Sarvaiya:** Investigation, Writing – review & editing. **Bharti Parmar:** Investigation, Methodology, Writing – review & editing. **Urvashi Chauhan:** Conceptualization, Investigation, Methodology.

Declaration of competing interest

The authors declare that they have no known competing financial interests or personal relationships that could have appeared to influence the work reported in this paper.

Data availability

No data was used for the research described in the article.

Availability of data and materials

Not Applicable.

References

[1] H. Bevrani, R. Feizi, S. Ataee, Robust frequency control in an islanded microgrid: and -synthesis approaches, IEEE Transaction on Smart Grid 7 (2015) 706–717, https://doi.org/10.1109/TSG.2015.2446984.

[2] K.S. Rajesh, S.S. Dash, R. Rajagopal, Load Frequency Control of Microgrid: a Technical Review, in: H Drück, J Mathur, V Panthalookaran, V Sreekumar (Eds.), Green Buildings and Sustainable Engineering, Springer Transactions in Civil and Environmental EngineeringSpringer, Singapore, 2020, https://doi.org/10.1007/978-981-15-1063-2_9.

[3] G. Hsieh, H. Hsieh, C. Tsai, C. Wang, Photovoltaic power increment-aided incremental-conductance MPPT with two-phased tracking, IEEE Trans. Power Electronics. 28 (2013) 2895–2911, https://doi.org/10.1109/TPEL.2012.2227279.

[4] R. Faraji, A. Rouholamini, H.R. Naji, R. Fadaeinedjad, M.R. Chavoshian, FPGA-based real time incremental conductance maximum power point tracking controller for PV systems, IET Power Electronics 7 (2014) 1294–1304, https://doi.org/10.1049/iet-pel.2013.0603.

[5] V.R. Kota, M.N. Bhukya, A novel linear tangents based P & O scheme for MPPT of a PV system, Renew. Sustain. Energy Rev. 71 (2017) 257–267, https://doi.org/10.1016/j.rser.2016.12.054.

[6] D. Sera, L. Mathe, T. Kerekes, S.V. Spataru, R. Teodorescu, On the perturb-and-observe and incremental conductance MPPT methods for PV systems, IEEe J. Photovolt. 3 (2013) 1070–1078, https://doi.org/10.1109/JPHOTOV.2013.2261118.

[7] A. Ahmed, L. Ran, J. Bumby, Perturbation parameters design for hill climbing MPPT techniques, in: IEEE Int. Symp. on Industrial Electronics, 28-31 May, 2012, https://doi.org/10.1109/ISIE.2012.6237368. Hangzhou, China.

[8] A. Frezzetti, S. Manfredi, A. Suardi, Adaptive FOCV-based control scheme to improve the MPP tracking performance: an experimental validation, IFAC Proceedings Volumes 47 (2014) 4967–4971, https://doi.org/10.3182/20140824-6-ZA-1003.02464.

[9] H.A. Sher, A.F. Murtaza, A. Noman, et al., A new sensorless hybrid MPPT algorithm based on fractional short-circuit current measurement and P&O MPPT, IEEe Trans. Sustain. Energy 6 (2015) 1426–1434, https://doi.org/10.1109/TSTE.2015.2438781.

[10] A.K. Rai, N.D. Kaushika, B. Singh, et al., Simulation model of ANN based maximum power point tracking controller for solar PV system, Solar Energy Mater. Solar Cells 95 (2011) 773–778, https://doi.org/10.1016/j.solmat.2010.10.022.

[11] M.A. Younis, T. Khatib, M. Najeeb, et al., An improved maximum power point tracking controller for PV systems using artificial neural network, Prz. Elektrotech. (Electrical Reviews). 3 (2012) 116–121.

[12] T.L. Kottas, Y.S. Boutalis, A.D. Karlis, New maximum power point tracker for PV arrays using fuzzy controller in close cooperation with fuzzy cognitive networks, IEEE Trans. Energy Convers. 21 (2006) 793–803, https://doi.org/10.1109/TEC.2006.875430.

[13] R. Rajesh, M.C. Mabel, Efficiency analysis of a multi-fuzzy logic controller for the determination of operating points in a PV system, Solar Energy 99 (2014) 77–87, https://doi.org/10.1016/j.solener.2013.10.036.

[14] N. Priyadarshi, A. Farooque, A.K. Sharma, et al., An adaptive neuro-fuzzy inference system-based intelligent grid-connected photovoltaic power generation, in: S Sahana, V Bhattacharjee (Eds.), Advances in Computational Intelligence. Advances in Intelligent Systems and Computing, Springer, Singapore, 2019, https://doi.org/10.1007/978-981-13-8222-2_1.

[15] K. Ishaque, Z. Salam, M. Amjad, et al., An improved particle swarm optimization (PSO)–based MPPT for PV with reduced steady-state oscillation, IEEE Trans. Power Electron. 27 (2012) 3627–3638, https://doi.org/10.1109/TPEL.2012.2185713.

[16] S. Mohanty, B. Subudhi, P.K. Ray, A new MPPT design using grey wolf optimization technique for photovoltaic system under partial shading conditions, IEEE Trans. Sustain. Energy. 7 (2016) 181–188, https://doi.org/10.1109/TSTE.2015.2482120.

[17] D.A. Nugraha, K.L. Lian, Suwarno, A novel MPPT method based on cuckoo search algorithm and golden section search algorithm for partially shaded PV system, Canadian J. Electr. Comput. Engg. 42 (2019) 173–182, https://doi.org/10.1109/CJECE.2019.2914723.

[18] K. Sundareswaran, V. Vigneshkumar, P. Sankar, et al., Development of an improved P&O algorithm assisted through a colony of foraging ants for MPPT in PV system, IEEE Trans. Ind. Inf. 12 (2016) 187–200, https://doi.org/10.1109/TII.2015.2502428.

[19] K. Sundareswaran, P. Sankar, P.S.R. Nayak, et al., Enhanced energy output from a PV system under partial shaded conditions through artificial bee colony, IEEE Trans. Sustain. Energy. 6 (2015) 198–209, https://doi.org/10.1109/TSTE.2014.2363521.

[20] M. Dashtdar, A. Flah, S.M.S. Hosseinimoghadam, A. El-Fergany, Frequency control of the islanded microgrid including energy storage using soft computing, Sci. Rep. 12 (2022), https://doi.org/10.1038/s41598-022-24758-6.

[21] G. Mallesham, S. Mishra, A.N. Jha, Ziegler-Nichols based controller parameters tuning for load frequency control in a microgrid, in: International Conference on Energy, Automation and Signal, 2011, https://doi.org/10.1109/ICEAS.2011.6147128, 28-30th DecemberBhubaneswar, India.

[22] Maneesh, Frequency control of a microgrid by using PI controller, in: International Conference on Energy, Power and Environment: Towards Sustainable Growth (ICEPE), 2015, https://doi.org/10.1109/EPETSG.2015.7510081, 12-13th JuneShillong, India.

[23] S. Oshnoei, A. Fathollahi, A. Oshnoei, M.H. Khoobanm, Microgrid frequency regulation based on a fractional order cascade controller, Fractal Fract. 7 (4) (2023) 343, https://doi.org/10.3390/fractalfract7040343.

[24] F. Habibi, H. Bevrani, J. Moshtag, Designing a self-tuning frequency controller based on ANNs for an isolated microgrid, Iran. J. Electr. Comput. Eng. 10 (2015) 88–95.

[25] S.M.S. Hosseinimoghadam, M. Dashtdar, H. Roghanian, Security control of islanded micro-grid based on adaptive neuro-fuzzy inference system, UPB Sci. Bull., Series C: Electr. Eng. Comput. Sci. 82 (2020) 189–204.

[26] E. Sahin, Design of an optimized fractional high order differential feedback controller for load frequency control of a multi-area multi-source power system with nonlinearity, IEEe Access. 8 (2020) 12327–12342.

[27] H.H. Ali, A.M. Kassem, M. Al-Dhaifallah, A. Fathy, Multi-verse optimizer for model predictive load frequency control of hybrid multi-interconnected plants comprising renewable energy, IEEe Access. 8 (2020) 114623–114642.

[28] A.H. Gomaa Haroun, Y.Y Li, Ant Lion optimized fractional order fuzzy pre-compensated intelligent pid controller for frequency stabilization of interconnected multiarea power systems, Appl. Syst. Innov. 2 (2) (2019) 17.

[29] A. Sobhy, H. Hasanien, A.Y. Abdelaziz, M. Ezzat, Manta ray foraging optimization algorithm-based load frequency control for hybrid modern power systems, IET Renw. Power Generat. 17 (2023) 1466–1487.

[30] J.R. Padhi, M.K. Debnath, S.K. Kar, Self-tuning Fuzzy-PI-controller for load frequency control analysis with the integration of wind energy, Energy Sources, Part A: Recov. Util. Environ. Effects. 44 (2022) 613–631, https://doi.org/10.1080/15567036.2022.2049928.

[31] A. Safari, F. Babaei, M.A. Farrokhifar, Load frequency control using a PSO-based ANN for micro-grids in the presence of electric vehicles, Int. J. Ambient Energy. 42 (2021) 688–700, https://doi.org/10.1080/01430750.2018.1563811.

[32] H. Bevrani, F. Habibi, P. Babahajyani, M. Watanabe, Y. Mitani, Intelligent frequency control in an AC microgrid: online PSO-based fuzzy tuning approach, IEEE Trans. Smart Grid. 3 (2012) 1935–1944, https://doi.org/10.1109/TSG.2012.2196806.

[33] A. Dev, B. Mondal, V. Verma, V. Kumar, Teaching learning optimization-based sliding mode control for frequency regulation in microgrid, Electric. Eng. (2024), https://doi.org/10.1007/s00202-024-02422-8.

[34] M.H. Khooban, T. Niknam, F. Blaabjerg, T. Dragičević, A new load frequency control strategy for micro-grids with considering electrical vehicles, Electric Power Syst. Res. 143 (2017) 585–598, https://doi.org/10.1016/j.epsr.2016.10.057.

[35] I. Eke, M. Saka, H. Gozde, Y. Arya, M. Taplamacioglu, Heuristic optimization based dynamic weighted state feedback approach for 2DOF PI-controller in automatic voltage regulator, Eng. Sci. Technol., Int. J. 24 (4) (2021) 899–910, https://doi.org/10.1016/j.jestch.2020.12.023.

[36] R. Choudhary, J.N. Rai, Y. Arya, Cascade FOPI-FOPTID controller with energy storage devices for AGC performance advancement of electric power systems, Sustain. Energy Technol. Assessments 53 (2022) 102671, https://doi.org/10.1016/j.seta.2022.102671. Part C.

[37] T. Kerdphol, F.S. Rahman, Y. Mitani, K. Hongesombut, S. Küfeoglu, Virtual inertia control-based model predictive control for microgrid frequency stabilization considering high renewable energy integration, Sustainability. 9 (5) (2017) 773, https://doi.org/10.3390/su9050773.

[38] VPSRVRS Sesha, S.S. Kesanakurthy, Model predictive control approach for frequency and voltage control of standalone micro-grid, IET Gen. Transm. Distrib. 12 (2018) 3405–3413, https://doi.org/10.1049/iet-gtd.2017.0804.

[39] M. Dashtdar, et al., Frequency control of the islanded microgrid based on optimised model predictive control by PSO, IET Renew. Power Gen. 16 (2022) 2088–2100, https://doi.org/10.1049/rpg2.12492.

[40] S. Rangi, S. Jain, Arya Yogendra, Utilization of energy storage devices with optimal controller for multi-area hydro-hydro power system under deregulated environment, Sustain. Energy Technol. Assess. 52 (2022) 102191, https://doi.org/10.1016/j.seta.2022.102191. Part C.
[41] M. Armin, et al., Robust extended control strategy using linear matrix inequality approach for islanded microgrid, IEEe Access. 8 (2020) 135883–135896, https://doi.org/10.1109/ACCESS.2020.3009188.
[42] H.M. Somarin, R Parvari, Micro-grid stabilizer design using sliding mode controller, Int. J. Electrical Power Energy Syst. 116 (2020), https://doi.org/10.1016/j.ijepes.2019.105519.
[43] M.I. Ibraheema, M. Edrisi, M. Gholipour, H.H Alhelou, A novel frequency regulation in islanded microgrid using sliding mode control with disturbance observers considering storages and EVs, Comput. Electric. Eng. 105 (2023), https://doi.org/10.1016/j.compeleceng.2022.108537.
[44] D. Deepika, S. Kaur, S. Narayan, Centralized sliding mode frequency regulation approach for an uncertain islanded micro grid integrated with disturbance observer, Asian J. Control 21 (2019) 2038–2048, https://doi.org/10.1002/asjc.1993.
[45] C. Wang, Y. Mi, Y. Fu, P Wang, Frequency control of an isolated micro-grid using double sliding mode controllers and disturbance observer, IEEe Trans. Smart. Grid. 9 (2016) 923–930, https://doi.org/10.1109/TSG.2016.2571439.
[46] A. Dev, S. Anand, U. Chauhan, V. Verma, V. Kumar, Frequency regulation in microgrid using sliding mode control with event- triggering mechanism, Electric. Eng. 106 (2023) 3381–3392, https://doi.org/10.1007/s00202-023-02141-6.
[47] K. Peddakapu, M.R. Mohamed, P. Srinivasarao, Y. Arya, P.K. Leung, D.J.K. Kishore, A state-of-the-art review on modern and future developments of AGC/LFC of conventional and renewable energy-based power systems, Renew. Energy Focus 43 (2022) 146–171, https://doi.org/10.1016/j.ref.2022.09.006.
[48] Y. Han, Modeling and Control of Power Electronic Converters for Microgrid Applications, Springer, Cham, 2022.
[49] H. Ramírez, R. Ortigoza, Controller Design Techniques in Power Electronics Devices, Springer-Verlag, London, 2006.
[50] B. Bandyopadhyay, F. Deepak, K.S. Kim, Sliding Mode Control Using Novel Sliding Surfaces, Springer, Berlin Heidelberg, 2009.
[51] A. Dev, V. Léchappé, M.K. Sarkar, Prediction-based super twisting sliding mode load frequency control for multi area interconnected power systems with state and input time delays using disturbance observer, Int. J. Control 94 (2019) 1751–1764, https://doi.org/10.1080/00207179.2019.1673487.
[52] W. Tan, S. Chang, R. Zhou, Load frequency control of power systems with non linearities, IET Generat., Transm. Distribut. 11 (2017) 4307–4313, https://doi.org/10.1049/iet-gtd.2017.0599.

Arkdev recieved his B. Tech. in Electronics & Instrumentation Engineering from WBUT Kolkata, West Bengal, India in 2013. He received his M. Tech in Power and Control System and PhD in Electrical Engineering from NIT Manipur, India in 2017 and 2021 respectively. He currently serves as an Assistant Professor at Faculty of Engineering & Technology, Parul Institute of Engineering & Technology, Parul University, Vadodara, Gujarat, India. His-research interests are sliding mode, higher order sliding mode control and its applications to power system studies, microgrid stability, event triggered control techniques. He has authored and co-authored various scientific articles in the field of sliding mode load frequency control.

Gautam Sarvaiya recieved his Bachelor's degree in Electrical Engineering from Atmiya Institute of Technology and Science, Rajkot, Gujarat, India in 2006. He received his M.Tech in Power Systems from School of Engineering, RK University, Rajkot, Gujarat India in 2014. He is currently working as an Assistant Professor at Lukhdhirji Engineering College, Morbi, Gujarat, India. His research interest includes load frequency control in power systems.

Bharti Parmar recieved her Bachelor's degree in Electrical Engineering from Lukhdhirji Engineering College, Morbi, Gujarat, India in 1999. She received her M.E. in Power Systems from Birla Vishvakarma Mahavidyalaya Engineering College, Vallabh Vidhyanagar, Gujarat, India in 2005. She is currently working as an Assistant Professor at Luckdhirji Engineering College, Morbi, Gujarat, India. Her research interest includes microgrid stability and renewable energy resources.

Urvashi Chauhan received her B.Tech degree in Electronics & Instrumentation Engineering from UPTU Lucknow in 2011. She has received M.Tech and PhD degree in Instrumentation and Control Engineering from Netaji Subhas Institute of Technology, University of Delhi in 2015 and 2022 respectively. Currently, she is working as Assistant Professor in the Department of Electronics and Communication Engineering, KCC Institute of Technology and Management, Greater Noida, Uttar Pradesh, India. Her research interests include renewable energy sources, solar energy, non-linear control and optimization techniques. She has authored and co-authored various scientific articles in the field of renewable energy sources.